

Improved defect-pool model for charged defects in amorphous silicon

M. J. Powell and S. C. Deane

Philips Research Laboratories, Redhill, Surrey, RH1 5HA, United Kingdom

(Received 8 March 1993; revised manuscript received 11 June 1993)

We have developed an improved defect-pool model for the calculation of the density of dangling-bond states in amorphous silicon. The results of this improved defect-pool model are contrasted with earlier work, from which we have eliminated some errors and approximations. We show that the calculated energy-dependent density of states depends on the specific microscopic reaction involving hydrogen, in contrast to previous conclusions. We calculate the bulk density of states, using the best input parameters drawn from experiment, and conclude that the best agreement with experimental results is found for a rather *wide* defect pool and for a microscopic model where *two* Si-H bonds break for every weak bond converted into *two* dangling bonds. The calculations predict that there are approximately four times as many charged defects as neutral defects in good-quality intrinsic amorphous silicon. We argue that this picture of the density of states is consistent with a wide range of experimental results. We show how this important conclusion depends on the principal parameters of the defect-pool model and investigate how the density of states would change with different parameters.

INTRODUCTION

There is now considerable experimental evidence that the density of states in amorphous silicon is dominated by amphoteric silicon dangling-bond states and that the density of these states is determined by a chemical equilibrium process.¹⁻³ The model for the defect-forming reaction involves the breaking of Si-Si bonds,⁴ which are generally thought to be stabilized by diffusive hydrogen motion through breaking and reforming Si-H bonds,^{3,5} although microscopic models that do not require hydrogen have been proposed.⁶ The equilibrium density of dangling-bond states depends on the Fermi energy, which leads to a higher density of dangling bonds in doped amorphous silicon than undoped amorphous silicon.^{1,7}

When the energy of the dangling-bond state can take a range of values, due to the inherent disorder of the amorphous network, then proper consideration of the chemical equilibrium model leads to an energy shift of the peak of the *formed* defects, due to the minimization of free energy. Furthermore, this energy shift is different for defects formed in the different charge states (+, 0, -). This is the so-called *defect-pool* model.⁸⁻¹⁰ For a sufficiently wide pool, the model leads to negatively charged defects in *n*-type amorphous silicon having a lower energy than positively charged defects in *p*-type amorphous silicon, even when the correlation energy is positive, a previously puzzling result found in many experiments.¹¹⁻¹³

The genesis of the defect-pool model lies in the work of Bar-Yam and Joannopoulos,¹⁴ who first pointed out that the formation energy of a defect depends on its charge state and that the difference in the formation energies depends on the Fermi energy and the energy of the defect itself. This paper predicted the essential result of the defect-pool model, but there was a problem with the number of potential defect sites and no obvious mechanism that allowed the whole Si network to rearrange its bonding.

Stutzmann⁴ introduced the weak-bond dangling-bond conversion model and Smith and Wagner¹⁵ identified the weak-bond energies with the valence-band-tail states, which are exponentially distributed in energy, giving a further distribution of formation energies. In a separate development, in Refs. 16-19 the importance of hydrogen in providing a mechanism for defect equilibration was proposed. This work was important in identifying possible microscopic mechanisms, but also in introducing additional entropy from the hydrogen reactions and so lowering the defect chemical potential.³ Strictly speaking, hydrogen is not part of the essential defect-pool model, but it is the only proposal to date that can provide a plausible microscopic mechanism with sufficient entropy to lower the defect chemical potential, and so give experimentally measured defect densities.

Winer brought together these different aspects in a classic paper, which defined the modern defect-pool model.²⁰ He calculated the density of states in undoped and doped *a*-Si:H and produced the key result that negatively charged defects in *n* type material were lower in energy than positively charged defects in *p* type material. However, Winer assumed that the density of states was dominated by defects of only one charge state in each type of material (negative in *n* type, positive in *p* type, and neutral in intrinsic). While this can be a good approximation in doped material, it is not a good approximation in intrinsic material.

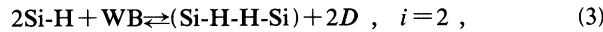
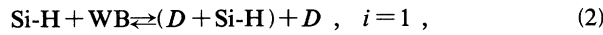
Schumm and Bauer extended this work by first considering the simultaneous formation of defects in all three charge states,²¹ but only later realized the importance of weak-bond depletion by defects of all three charge states.²² Their results showed more charged defects than neutral defects in intrinsic *a*-Si:H. Branz and Silver²³ also concluded there were more charged defects than neutral defects, with a model having some similarities, but expressed in terms of potential fluctuations. However, Branz and Silver²³ did not include weak-bond

dangling-bond conversion nor did they include any hydrogen entropy in their model. Schumm and Bauer considered different microscopic reactions, with zero, one, or two Si-H bonds mediating the weak-bond-breaking process, but concluded that the extra entropy only affected the absolute densities of states formed and not their energy spectrum.^{21,22}

In this paper, we present an improved defect-pool model. We show that the energy spectrum of the density of states *does* depend on the number of Si-H bonds mediating the weak-bond-breaking reaction. We calculate the density of states and derive a simple expression for the energy separation of positively and negatively charged defects. We investigate how the density of states depends on the principal parameters of the defect-pool model. We conclude that the best agreement with experimental results is obtained for a rather wide defect pool and for a model where two Si-H bonds mediate the weak-bond-breaking reaction.

IMPROVED DEFECT-POOL MODEL

The general principle of the model is that dangling bonds are formed by the breaking of weak Si-Si bonds and that the density of these is determined by a chemical equilibrium between the weak bonds and the dangling bonds. We can consider the dangling bonds to be formed by one of three different microscopic chemical reactions, depending on how many Si-H bonds are involved in the process:³



where i indicates the number of Si-H bonds mediating the weak-bond-breaking chemical reaction. Here the parentheses indicate species which are intimately connected and cannot diffuse apart. These are the same reactions considered by Street and Winer.³ For $i=0$, the

weak bond is broken, but the dangling bonds cannot move apart without the involvement of hydrogen diffusion. For $i=1$, one Si-H bond is broken and the hydrogen atom diffuses to the weak-bond site, breaking the weak bond. The defect in the $(D + \text{Si-H})$ is labeled D_w in the Street and Winer notation and the D defect is labeled D_H . For $i=2$, a second Si-H bond is broken, resulting in a doubly hydrogenated weak-bond site and two isolated D defects.

To calculate the defect density, we first determine a general expression for the defect chemical potential,²⁴ which is defined as the free-energy change upon adding one extra defect to the system. The defect chemical potential for the amphoteric dangling-bond defect contains three terms; the energy of the electron (or electrons) of the defect, the entropy associated with the electron occupancy of the defect, and the additional entropy associated with the location of the defect on alternative hydrogen sites. We now calculate each of these in turn.

The mean energy of the electrons in the dangling-bond state depends on the probability of the dangling bond being in each of its three charge states. If the defect is positively charged, then the defect's electron has been removed to the Fermi level, E_F . If the defect is neutral, then the defect's electron is at the defect energy, E . If the defect is negatively charged, then an extra electron has to be moved from the Fermi level to the defect, giving a total energy of $2E - E_F + U$. The extra energy U is the correlation energy, which is needed to place two electrons on the same defect. The mean energy of the electrons is therefore given by

$$\langle e \rangle = E_F f^+(E) + E f^0(E) + [2E - E_F + U] f^-(E), \quad (4)$$

where the functions f^+ , f^0 , and f^- are the occupancy functions of the amphoteric dangling bond in each charge state, i.e., occupied by zero, one, or two electrons, respectively. These occupancy functions can easily be calculated from statistical mechanics²⁵ and are shown to be given by²⁶

$$f^+(E) = \frac{1}{1 + 2 \exp([E_F - E]/kT) + \exp([2E_F - 2E - U]/kT)}, \quad (5)$$

$$f^0(E) = \frac{2 \exp([E_F - E]/kT)}{1 + 2 \exp([E_F - E]/kT) + \exp([2E_F - 2E - U]/kT)}, \quad (6)$$

$$f^-(E) = \frac{\exp([2E_F - 2E - U]/kT)}{1 + 2 \exp([E_F - E]/kT) + \exp([2E_F - 2E - U]/kT)}. \quad (7)$$

Remember that E is the energy of the amphoteric dangling-bond state, with the $+/0$ transition being at an energy E and the $0/-$ transition being at $E + U$.

The electron entropy is given by the Boltzmann definition,²⁷ $s = -\sum p_i \ln p_i$, where p_i is the probability of the system being in any one state and the summation is over all accessible states. For the case of the dangling-bond defect, this gives

$$s_e = -\{f^+(E) \ln f^+(E) + 2[f^0(E)/2] \ln (f^0(E)/2) + f^-(E) \ln f^-(E)\}, \quad (8)$$

where the factors of 2 associated with the neutral charge state are due to the spin degeneracy of that state. The total entropy is zero if the defect is positively or negatively charged, i.e., $f^+ = 1$ or $f^- = 1$. If the defect is neutral,

then $s = -\ln \frac{1}{2}$, which makes the neutral defect twice as likely to form than would be expected on purely energetic grounds.

We can add the terms from (4) and (8) to give the defect chemical potential, without hydrogen entropy, $\mu_d = \langle e \rangle - kTs_e$;

$$\mu_d(E) = f^+ [E_F + kT \ln f^+(E)] + f^0 [E + kT \ln(f^0(E)/2)] + f^- [2E - E_F + U + kT \ln f^-(E)]. \quad (9)$$

By rearranging the occupancy functions (5)–(7), it can be shown that the three terms in square brackets in Eq. (9) are identical, and since $f^+ + f^0 + f^- = 1$, then,

$$\begin{aligned} \mu_d(E) &= E_F + kT \ln f^+(E) \\ &= E + kT \ln(f^0(E)/2) \\ &= 2E - E_F + U + kT \ln f^-(E). \end{aligned} \quad (10)$$

Figure 1 shows a plot of μ_d as a function of the defect energy, for three Fermi levels. When $f^+ \approx 1$, then $\mu_d \approx E_F$; when $f^- \approx 1$, then $\mu_d \approx 2E - E_F + U$; but when $f^0 \approx 1$, then $\mu_d \approx E - kT \ln(2)$. This can be compared with the expression for the neutral defect chemical potential used by Winer,²⁰ $\mu_d = E$.

Next, we consider the effect of hydrogen involvement in the chemical reactions (1)–(3). In these reactions i of the defects are swapped to hydrogen sites distant from the original broken weak bond, where $i=0, 1$, or 2 . The chemical reactions (2) and (3) add extra entropy to the defect chemical potential, since the defects can gain entropy by swapping hydrogen from Si-H bonds, transferring the defect to a distant Si-H site. There are several orders of magnitude more hydrogen sites than there are defects, so a large amount of entropy becomes available from the choice of which distant hydrogen site contains the defect. It is important to realize, however, that a defect at an energy E gains entropy only from those Si-H sites that would also form a defect at the *same* energy, E .

Consider a hydrogen site (a Si-H bond) which would form a dangling-bond defect at energy E , if the hydrogen

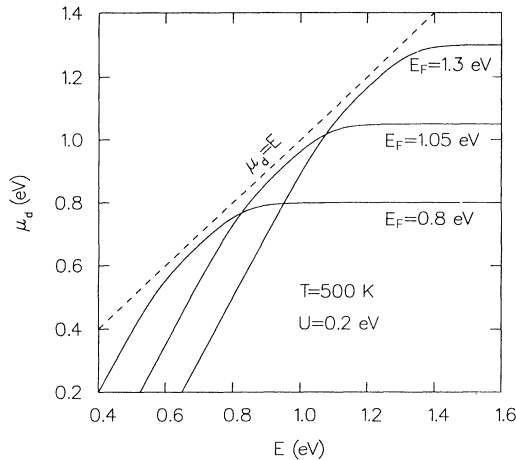


FIG. 1. The defect chemical potential (without hydrogen entropy), μ_d , as a function of defect energy, E , for three different Fermi-level positions. The valence-band mobility edge is taken as the energy reference, i.e., $E_v = 0$ eV. The dashed line indicates the electron energy for the neutral defect ($\langle e \rangle = E$).

atom were removed. The number of these sites is $HP(E)$, where H is the total concentration of hydrogen and $P(E)$ is the energy distribution of sites which would form defects at energy E (the defect-pool function). The *probability* that a defect exists at any given hydrogen site is given by $p_d = iD(E)/[2HP(E)]$, where $D(E)$ is the density of defects at energy E . The $i/2$ term comes from the fact that for every two defects formed only i of these can swap hydrogen from distant sites, according to the reactions (1)–(3). The *total* entropy can then be calculated from $s_H = -\sum p_d \ln(p_d)$, where we sum over $HP(E)$ hydrogen sites, with identical p_d . Then, dividing by the density of defects $D(E)$, we get the hydrogen entropy *per defect* at energy E , to be

$$s_H = -\frac{i}{2} \ln \left[\frac{iD(E)}{2HP(E)} \right]. \quad (11)$$

Adding this entropy to Eq. (10) leads to a general expression for the defect chemical potential,

$$\mu_d(E) = E + kT \ln \left[\frac{f^0(E)}{2} \right] + \frac{ikT}{2} \ln \left[\frac{iD(E)}{2HP(E)} \right]. \quad (12)$$

This same result can also be deduced by applying the law of mass action directly to each of the chemical reactions (1)–(3), but some care is needed to avoid errors and account for the entropy and electron occupancy correctly.

To calculate the defect density at energy E , we now write down the probability of converting a weak-bond state at energy E_t , remembering that a weak bond forms two dangling bonds and accounting for the depletion of the weak-bond states by the formed defects:

$$D(E) = [P(E)g_t(E_t) - D(E)] \exp\{-2[\mu_d(E) - E_t]/kT\}, \quad (13)$$

where $P(E)g_t(E_t)$ is the density of weak bonds at energy E_t that lead to potential defect sites at an energy E .

Here we adopt the common assumption that the formation energy for the weak-bond to dangling-bond conversion can be represented by the one-electron energy differences of these states.¹⁵ This assumption neglects ionic relaxation and multielectron contributions to the formation energy, for which some justification has been given.^{15,20} Later in this paper, we further justify this approximation from the numerical results.

It is also important to note that in (13) the energy of *both* defects is E . This is correct, since the two defects minimize their free energy *independently* and will, on average, have the same energy. It is not correct to give the defects statistically independent energies, as was done by Schumm and Bauer,²² since this leads to minimizing the free energy of a *pair* of defects, which could only be a correct physical interpretation if the two defects were intimately paired. This may be a reasonable interpretation for $i=0$, but not for the models with $i=1$ and 2 , which imply long-range hydrogen diffusion, leading to separation of the two defects by an arbitrarily large distance. Essentially, the choice of minimizing the defect free energy independently or in pairs corresponds to *different* microscopic models. For the case of $i=0$, this corresponds

to assuming either that the defects formed from the same weak bond have the same energy, or that they have statistically independent energies, respectively.

The $D(E)$ in (13) gives the density of states formed from weak-bond states at energy E_t , so if there is a distribution of weak-bond energies, then we must write (13) in integral form, where the integral is over the weak-bond energies;

$$D(E) = \int \frac{P(E)g_t(E_t)}{1 + \exp\{2[\mu_d(E) - E_t]/kT\}} dE_t. \quad (14)$$

We identify the weak-bond states with the valence-band-tail states, which are exponentially distributed in energy,¹⁵ $g_t(E_t) = N_{v0} \exp([E_v - E_t]/E_{v0})$, where N_{v0} is the density of tail states extrapolated to the valence-band mobility edge, E_v , and E_{v0} is the characteristic energy of the exponential. The integral (14) can be evaluated exactly,²⁸ but here we use the approximation that for $\mu_d < E_t$ all weak-bond states convert, while for $\mu_d > E_t$ a Boltzmann fraction of states converts,¹⁰ which leads to

$$D(E) = P(E)N_{v0} \frac{2E_{v0}^2}{2E_{v0} - kT} \exp\left(\frac{-\mu_d(E)}{E_{v0}}\right). \quad (15)$$

The defect-pool function $P(E)$ is assumed to have a Gaussian distribution,

$$P(E) = \frac{1}{\sigma\sqrt{2\pi}} \exp\left(\frac{-[E - E_p]^2}{2\sigma^2}\right), \quad (16)$$

where σ is the pool width and E_p is the most probable energy in the distribution of available sites for defect formation. If the expression for μ_d from (12) is substituted into (15), then after suitable rearrangement we get

$$D(E) = \gamma \left[\frac{2}{f^0(E)} \right]^{\rho kT/E_{v0}} P\left[E + \frac{\rho\sigma^2}{E_{v0}}\right], \quad (17)$$

with

$$\gamma = \left[\frac{N_{v0}2E_{v0}^2}{[2E_{v0} - kT]} \right]^\rho \left[\frac{i}{2H} \right]^{\rho-1} \times \exp\left[\frac{-\rho}{E_{v0}} \left[E_p - E_v - \frac{\rho\sigma^2}{2E_{v0}} \right] \right], \quad (18)$$

where $\rho = 2E_{v0}/(2E_{v0} + ikT)$. Note that $[i/2H]^{\rho-1} = 1$ for $i=0$. These formulas express the density of states at *equilibrium*, which is maintained for temperatures above the equilibration temperature, T^* . To calculate $D(E)$ at lower temperatures, we must use the values at T^* for the parameters in Eqs. (17) and (18). In particular, we should replace E_{v0} by E_{v0}^* , E_F by E_F^* , and T by T^* , where the asterisk indicates the value of a temperature-dependent parameter at the equilibration temperature. $D(E)$ is not a function of temperature below T^* , since the equilibrium density of states is assumed to be *frozen-in*.

The energy dependence of the density of states comes from Eq. (17). The absolute density is given by the scaling factor γ , in Eq. (18). The energy dependence of the density of states depends on i through ρ . Since $P(E)$ is a Gaussian, Eq. (17) shows a shifted Gaussian, modified by

the term containing the occupancy for neutral defects $f^0(E)$. Since $f^0(E)$ is a symmetrical function with an exponential energy dependence at high and low energy, its effect on the density of states is large, leading to extra features in $D(E)$ at higher and lower energy. $D(E)$ is no longer a simple Gaussian.

CALCULATED DENSITY OF STATES

We now calculate the density of states, using the best available input parameters, drawn from experimental results. We take the following values for parameters: $N_{v0} = 2 \times 10^{21} \text{ cm}^{-3} \text{ eV}^{-1}$,²⁹ $H = 5 \times 10^{21} \text{ cm}^{-3}$ (i.e., 10% hydrogen content), and $T^* = 500 \text{ K}$.^{10,20} The band gap (mobility gap) is $E_g = 1.9 \text{ eV}$ (Ref. 30) and the intrinsic Fermi level is set at $E_F - E_v = 1.05 \text{ eV}$ to give a conduction activation energy of $E_c - E_F = 0.85 \text{ eV}$. We allow for a temperature dependence of the valence-band-tail slope by using the relationship $E_{v0}^2 = E_{v0}^2(T=0) + (kT)^2$.³¹ We take $E_{v0} = 0.036 \text{ eV}$ at $T=0 \text{ K}$, which gives a room-temperature valence-band slope of 0.045 eV (typical for good quality material³²) and a value of 0.056 eV at the equilibration temperature.

The correlation energy is not known very accurately. Early measurements of U (Refs. 33–35) relied on the assumption that the energy dependence of the density of states does not change with doping, which is clearly not correct in a defect-pool model. Certainly from the low-temperature dependence of the spin density, U is positive and must be greater than 0.1 eV (Ref. 35) [recent measurements give $U = 0.2\text{--}0.3 \text{ eV}$ (Ref. 36)]. In this paper, we have taken the commonly used value of $U = 0.2 \text{ eV}$.^{20,22}

The key parameter σ , the width of the defect pool, is set at $\sigma = 0.178 \text{ eV}$, with $i=2$. This value is chosen to give the experimentally determined energy separation between negatively charged defects in *n*-type *a*-Si:H and positively charged defects in *p*-type *a*-Si:H, which we label Δ . We take the value for this energy separation as $\Delta = 0.44 \text{ eV}$, which is found from our recent field-effect conductance measurements.³⁷ This is in good agreement with reported values of 0.4–0.5 eV from luminescence measurements,^{13,38} photomodulation spectroscopy,³⁹ and optical absorption,¹¹ while the value for this energy difference from photoemission measurements is 0.7 (± 0.2) eV.⁴⁰ We consider the effect of changing various parameters of the defect-pool model later.

Figure 2 shows the calculated density of dangling-bond states, $D(E)$, in *a*-Si:H. We believe this gives a good representation of the density of states in good quality intrinsic *a*-Si:H. The density of states is *frozen-in* at the equilibration temperature, $T^* = 500 \text{ K}$. We show $D(E)$ divided into components of different charge density, D^+ , D^0 , and D^- , defined by,

$$\begin{aligned} D^+(E) &= D(E)f^+(E), \\ D^0(E) &= D(E)f^0(E), \\ D^-(E) &= D(E)f^-(E), \end{aligned} \quad (19)$$

at three different temperatures. The shifted Gaussian

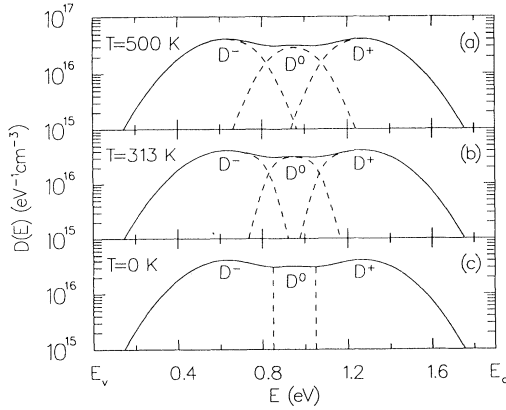


FIG. 2. The calculated density of dangling-bond states, $D(E)$, in intrinsic a -Si:H. The density of states is frozen in at the equilibration temperature $T^*=500$ K and the Fermi level is at $E_F=1.05$ eV. The total density of states $D(E)$ is shown divided into components of D^- , D^0 , and D^+ , at the equilibration temperature $T=500$ K (a); at a typical measurement temperature $T=313$ K (b); and at $T=0$ K (c).

from Eq. (17) is centered on the D^0 states, while the peaks in $D(E)$ at higher and lower energy consist of D^- and D^+ states, which are present even in intrinsic material. Of course the total density of states $D(E)$ does not change with T , because this only depends on T^* , which is fixed, but f^+ , f^0 , and f^- are a function of temperature. At zero temperature, all states above E_F are D^+ , all states below $E_F - U$ are D^- , and all states in between are D^0 . For intrinsic a -Si:H, the position of E_F gives an equal number of D^+ and D^- states and charge neutrality is maintained. E_F is not temperature dependent. The total density of defects is $4.0 \times 10^{16} \text{ cm}^{-3}$, while the density of neutral defects is 8.3×10^{15} at 500 K, 7.4×10^{15} at 313 K, and 6.2×10^{15} at zero T.

The energy separation between the peak of the negatively charged defects and the positively charged defects is $2\rho\sigma^2/E_{v0}=0.64$ eV, but remember this refers to the $+/0$ transition energy of both states. The energy separation between the doubly occupied D^- state and the empty D^+ state is given by $\Delta=2\rho\sigma^2/E_{v0}-U=0.44$ eV.²⁴ The relationship between E_F and E_p is given by $E_p=E_F+\Delta/2$ and so the peak of the D^+ states coincides with E_p .

One-electron density of states

It is extremely useful to map the density of states $D(E)$ onto an effective one-electron density of states $g(E)$, which relates well to the density of states that is measured in most spectroscopic techniques with thermal transitions, like the field effect,^{37,41} space-charge-limited current analysis,⁴² and deep-level transient spectroscopies (DLTS).^{43,44} The occupancies of correlated dangling-bond states are given by f^+ , f^0 , and f^- , whereas the occupancy of one-electron states is given by the Fermi-Dirac function. If $U=0$, we can write $g(E)=2D(E)$. Alternatively, provided U is larger than about $3kT$, we

can approximate $g(E)$ by

$$g(E) \approx D(E + kT \ln(2)) + D(E - U - kT \ln(2)), \quad (20)$$

where the $kT \ln(2)$ term comes from the spin degeneracy of the singly occupied state. This is not exact, but it is a very good approximation, leading only to a small error of about $\exp(-U/kT)$ in the density.

Figure 3 shows the effective one-electron density of states for intrinsic a -Si:H, for the same $D(E)$ in Fig. 2, also adding contributions from exponential conduction- and valence-band-tail states. From Eq. (20), we see that $g(E)$ depends on T , even when $D(E)$ does not. In Fig. 3, $g(E)$ is plotted at $T=313$ K. The components of $g(E)$ are shown in their charge state at the equilibration temperature. We adopt our earlier notation,⁴¹ and label as D_e those states that are formed as D^- states at equilibrium, while D_h are states formed as D^+ . We adopt a new notation for the states formed as D^0 , labeling them D_z (in Ref. 41, we labeled these states D_0). This is useful, since we can more clearly distinguish between contributions to $g(E)$ from the $+/0$ one-electron transition energies and the $0/-$ one-electron transition energies. This means that there are six components in the total one-electron density of states, $g(E)$, and all of these states would be detected in experiments where $g(E)$ is probed by moving the Fermi level through a frozen-in density of states. Thus, a D_e^+ state means a state formed as a negatively charged defect at equilibration, which has subsequently lost two electrons, as the Fermi level is swept to lower energies without reequilibration of the density of states $D(E)$.

On a one-electron density-of-states diagram, the energy separation between the $+/0$ and $0/-$ transition energies is $U_{\text{eff}}=U+2kT \ln(2)$, and in Fig. 3 the energy separation between the D_e^- and the D_h^+ levels is given by $\Delta'=2\rho\sigma^2/E_{v0}-U_{\text{eff}}=0.40$ eV, with E_F midway between. These are the energies that would be measured in experiments with thermal transitions, which are interpreted using a one-electron density of states, like the field effect and most spectroscopic techniques, like DLTS. However-

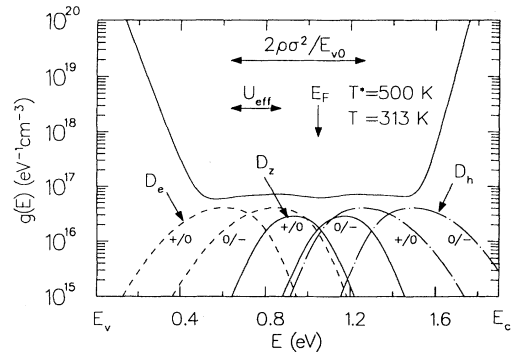


FIG. 3. The effective one-electron density of states in a -Si:H, $g(E)$, at $T=313$ K, for the same $D(E)$ shown in Fig. 2. The components of $g(E)$ are shown as states formed at the equilibration temperature, $T^*=500$ K. D_e states (dashed lines) are states formed as D^- , D_h states (chain lines) are states formed as D^+ , and D_z states (solid lines) are states formed as D^0 .

er, experiments which probe optical transitions involving amphoteric states can really only be interpreted using the correct statistics, where the real energy separation between the $+/0$ and $0/-$ transitions is U .

In Fig. 3, we observe the very interesting result that the total density of one-electron states, $g(E)$, is almost independent of energy (for intrinsic material with no band bending), even though the states have been formed from a *single* pool with a Gaussian width parameter σ of only 0.178 eV. The $+/0$ and $0/-$ transition energies are not resolved. This gives some justification for the old procedure of modeling the one-electron density of states as conduction- and valence-band-tail states, plus an energy-independent density of deep states.⁴⁵

Doped amorphous silicon

Figure 4 shows the calculated density of states $D(E)$ for lightly doped amorphous silicon. The equilibrium Fermi level E_F^* is shifted by 0.25 eV, from the intrinsic position. There is a temperature dependence of the Fermi level in doped material, due to the statistical shift to conserve the total charge. The statistical shift consists of two opposing terms due to charge in the tail states and charge in the deep states. For our model, the statistical shift nearly cancels for *n*-type material, giving $E_F = E_F^* - 0.006$ eV, at 313 K, but the statistical shift is dominated by the deep states for *p*-type material, giving $E_F = E_F^* + 0.021$ eV. The components of D^- , D^0 , and D^+ , are shown at $T=313$ K, including this statistical shift.

Figure 5 shows the one-electron density of states, for lightly doped material, at $T=313$ K, but with the equilibrium ($T^*=500$ K) components D_e , D_z , and D_h indicated. Note that in *n*-type material, the peak position of the D_e states remains the same, but the peak position of the D_z and D_h states is shifted to a higher energy, compared to their position in intrinsic material. The density of D_z states is also decreased. In *p*-type material, the position

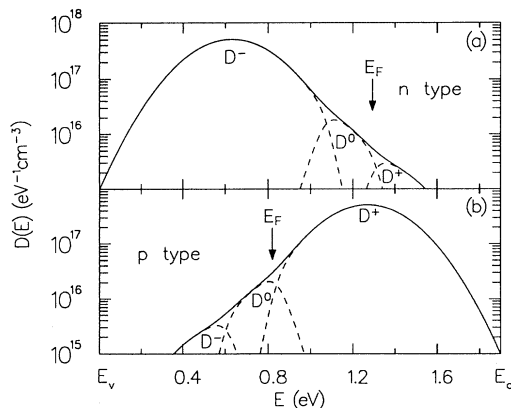


FIG. 4. The calculated density of dangling-bond states, $D(E)$, in lightly doped *a*-Si:H. The equilibrium Fermi level E_F^* is shifted by 0.25 eV from its position in intrinsic *a*-Si:H; *n* type (a) and *p* type (b). The density of states is frozen in at $T^*=500$ K. The D^- , D^0 , D^+ components and E_F are shown at $T=313$ K.

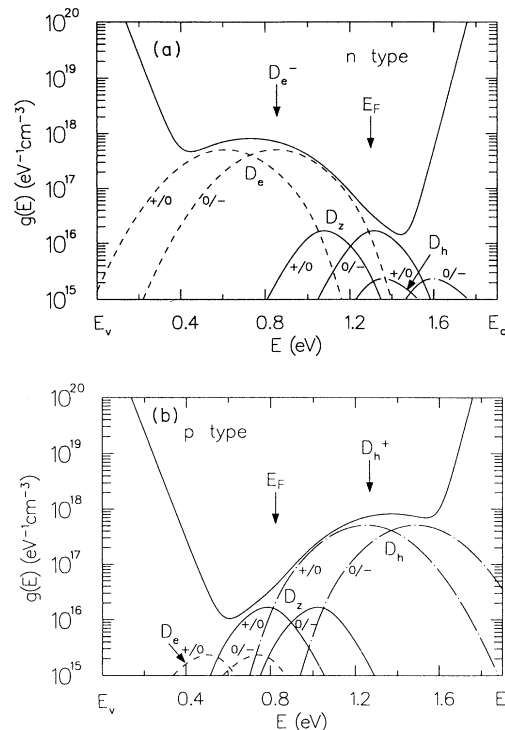


FIG. 5. The effective one-electron density of states, $g(E)$, for lightly doped *a*-Si:H. The Fermi level is shifted by 0.25 eV from its position in intrinsic *a*-Si:H; *n* type (a) and *p* type (b). The components of $g(E)$ are shown as states formed at the equilibration temperature, $T^*=500$ K.

of the D_h states remains the same, while the D_z and D_e states move to lower energy. However, the energy separation of the D_e^- state in *n*-type material from the D_h^+ state in *p*-type material is still given by $\Delta' = 2\rho\sigma^2/E_{v0} - U_{\text{eff}} = 0.4$ eV. This is a different picture than we presented previously,⁴¹ by extending the Winer²⁰ model, where the position of all D_e , D_z , and D_h components remained the same and the energy shift between D_e^- and D_h^+ was $2\sigma^2/E_{v0} - U$.

Figure 6 shows the Fermi-level dependence of the equilibrium density of D_e , D_z , and D_h states integrated over energy. The total density of states D_{tot} increases ex-

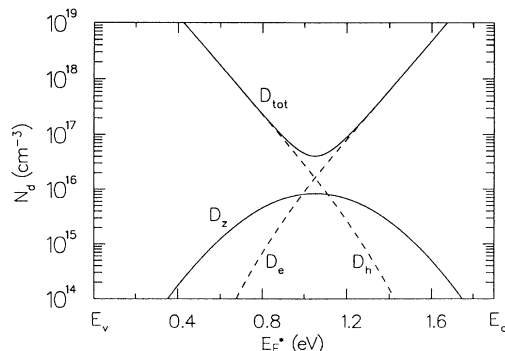


FIG. 6. The density of D_e , D_z , and D_h states (formed at the equilibration temperature), as a function of the Fermi-level position at equilibration, E_F^* .

ponentially as the Fermi level is displaced from midgap and is dominated by D_e states for n -type material and by D_h states for p -type material. When the total density of states is dominated by one type of defect (D_e for n type and D_h for p type), then the Fermi-level dependence of the total density of states can be determined, from Eq. (17), to be given by

$$D_e \sim \exp(\rho E_F / E_{v0}), \quad (21)$$

$$D_h \sim \exp(-\rho E_F / E_{v0}). \quad (22)$$

Thus the density of states increases exponentially with the shift in E_F , with a characteristic energy of $E_{v0}/\rho = E_{v0} + ikT/2$. For the parameters in our model, this characteristic energy is 99 meV, which is in excellent agreement with the experimental results of Pierz, Fuhs, and Mell¹³ for n -type a -Si:H. For p -type a -Si:H, Pierz, Fuhs, and Mell¹³ find a lower characteristic energy due to the additional effect of E_{v0} increasing with impurity doping. This latter effect is also observed for higher levels of n -type doping and is presumed to be due to extra disorder in the presence of dopant atoms.

The key result in Fig. 6 is that charged defects outnumber the neutral defects, even for intrinsic amorphous silicon, with the ratio of charged to neutral defects at equilibrium, $(D_e + D_h)/D_z = 3.9$.

EFFECT OF DEFECT-POOL PARAMETERS

We now consider the effect of altering the input parameters of the defect-pool model, in particular on the calculated ratio of charged to neutral defects. Figure 7 shows the calculated equilibrium ratio of charged to neutral defects, as a function of the width of the defect pool, σ , for various choices of the other fixed parameters. For our original choice of the other fixed parameters (bold line in Fig. 7), the density of charged defects exceeds the density

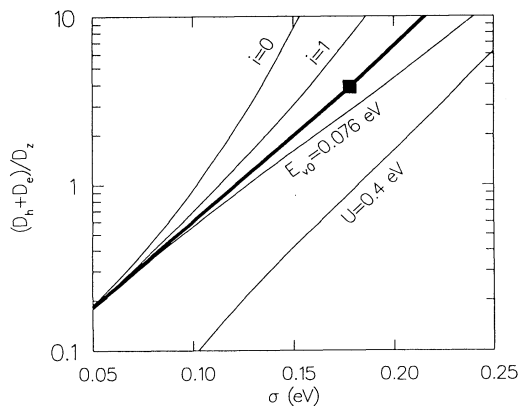


FIG. 7. Calculated ratio of charged to neutral defects, at the equilibration temperature, $[D_e + D_h]/D_z$, as a function of the width of the defect pool, σ , for different choices of fixed parameters. The solid square indicates the choice of parameters used in Figs. 2–6 ($E_F = 1.05$ eV, $E_{v0} = 0.56$ eV, $U = 0.2$ eV, $i = 2$, with $\sigma = 0.178$ eV). The solid curve indicates the effect of varying σ only. The other curves indicate the effect of varying one other parameter, as labeled.

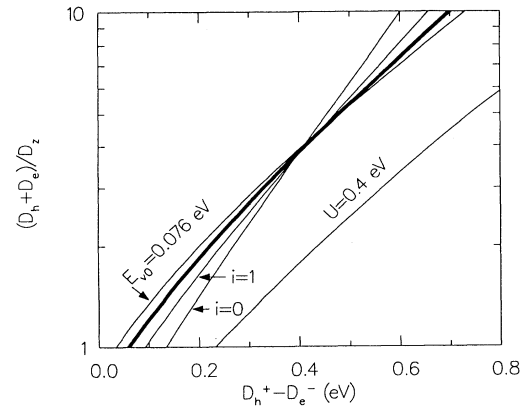


FIG. 8. Calculated charged to neutral defect ratio, at the equilibration temperature, $[D_e + D_h]/D_z$, plotted against the one-electron energy separation, $D_h^+ - D_e^-$, at 313 K, for different choices of fixed parameters. For each curve, E_F , E_{v0} , U , and i are fixed at the same values as in Fig. 7 and σ is varied.

of neutral defects, for σ greater than 0.12 eV. Microscopic models which decrease the value of i lead to higher ratios, while reducing E_{v0} also leads to higher ratios. However, increasing U leads to lower ratios. For $U = 0.4$ eV, and the same values for the other parameters, then the ratio of charged to neutral defects is reduced to 0.9.

Figure 8 shows the same results in Fig. 7, but plotted as a function of the one-electron energy separation, $\Delta' = D_h^+ - D_e^-$, at 313 K. For each curve, E_F , E_{v0} , U , and i are fixed and σ is varied. The results show that for $U = 0.2$ eV, the ratio of charged to neutral defects remains approximately constant at about 4, for any combination of parameters that keep the energy separation $D_h^+ - D_e^- \approx 0.4$ eV. The ratio of charged to neutral defects does depend on U , even for a given energy separation, $D_h^+ - D_e^-$. For $U = 0.4$ eV and maintaining a 0.4-eV energy separation for $D_h^+ - D_e^-$, the ratio of charged to neutral defects is nearer to 2.

Figure 9 shows the effect of altering the parameter i on

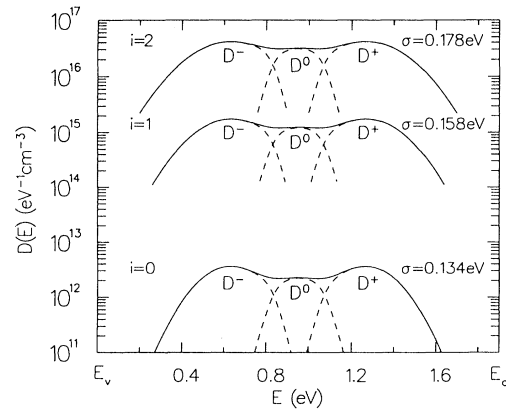


FIG. 9. Calculated density of dangling-bond states, $D(E)$, for the model with different values of i (number of Si-H bonds mediating the weak-bond breaking reaction); σ is adjusted to maintain the energy separation $D_h^+ - D_e^-$. The D^- , D^0 , and D^+ components are shown at $T = 313$ K.

the density of states $D(E)$. In contrast to the conclusions of Schumm and Bauer,^{21,22} altering i changes the *energy spectrum* of the density of states, as well as their absolute density. In Fig. 9, we adjust the value of σ to keep the energy separation of the D^- and D^+ states constant. This leads to a reduction of σ to 0.158 eV for $i=1$ and 0.134 eV for $i=0$. The total density of states is reduced dramatically, by changing i , with D_{tot} values of $1.6 \times 10^{15} \text{ cm}^{-3}$ for $i=1$ and $2.9 \times 10^{12} \text{ cm}^{-3}$ for $i=0$, compared to $4.0 \times 10^{16} \text{ cm}^{-3}$ for $i=2$. The ratio of charged to neutral defects does not change significantly and the calculated density of spin active defects (D^0), at $T=313 \text{ K}$, is $2.4 \times 10^{14} \text{ cm}^{-3}$ for $i=1$ and $5.3 \times 10^{11} \text{ cm}^{-3}$ for $i=0$, compared to $7.4 \times 10^{15} \text{ cm}^{-3}$ for $i=2$. The number of D^0 states for $i=2$ is much closer to the number of spins found experimentally in good quality intrinsic $a\text{-Si:H}$.⁴⁶

Furthermore, we argue that i must equal 2, if the system attains true chemical equilibrium. For any situation where an $i=1$ reaction occurs, then an $i=2$ reaction must also be possible, as both depend on the diffusion of hydrogen. The $i=2$ reaction will completely dominate the resulting density of states, as shown in Fig. 9. Since the calculated density of defects for $i=2$ gives a good agreement with experiment, we take this as good justification for the defect formation energies being given by the one-electron energy differences¹⁵ and that lattice relaxation energies are indeed negligible.

The alternative is that $i=0$, and then the only way that large enough defect densities can occur is if there is a very large local lattice relaxation energy or if the dangling bonds can diffuse to different Si sites, without hydrogen motion, giving entropy from the choice of Si sites.¹⁵ However, there is little experimental evidence for this view and significant evidence for the role of hydrogen and so we adopt the hydrogen model, with $i=2$.

DENSITIES OF STATES FOR DIFFERENT POOLS

Although we believe the density of states shown in Figs. 2–6 gives the best picture of the density of states in good quality amorphous silicon, the results do depend on the choice of two critical parameters, which are not well established by independent experimental results, namely, σ and U . Nevertheless, we believe the improved defect-pool model to be valid, regardless of the choice of these

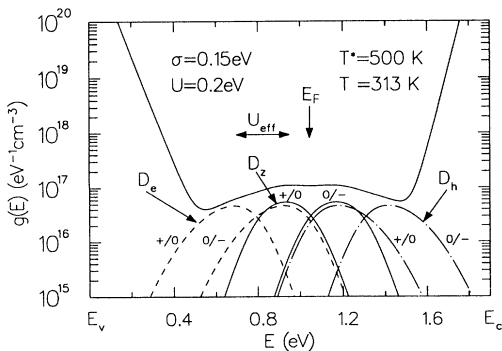


FIG. 10. One-electron density of states, $g(E)$, for a model with a narrower defect pool, $\sigma=0.15 \text{ eV}$.

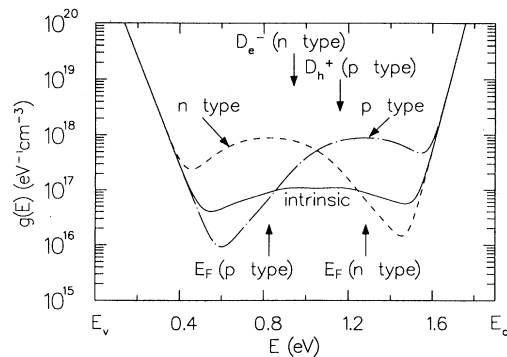


FIG. 11. One-electron density of states for lightly doped material with a narrow pool, $\sigma=0.15 \text{ eV}$.

parameters. Therefore, in this section we calculate the density of states for two different choices of σ and U to highlight the effect that these different choices would have on the results. We use the same values for the other input parameters and keep $i=2$, since the above arguments for $i=2$ are generally valid.

Figures 10 and 11 show the one-electron density of states, calculated for $\sigma=0.15 \text{ eV}$ and $U=0.2 \text{ eV}$. For this value of σ , the total number of defects in *each* charge state is identical, in intrinsic material, which means that the ratio of charged to neutral defects is 2 (Fig. 12). Note that in Fig. 10 the peak density of the D_z states is slightly higher than the D_e or D_h states, since the peak shapes are different. The energy separation between D_e^- (in n type) and D_h^+ (in p type) would be 0.22 eV, which is less than found experimentally.

Figures 13–15 show the equivalent diagrams for the case where $\sigma=0.1 \text{ eV}$ and $U=0.4 \text{ eV}$. In this situation, the $+/0$ and $0/-$ transitions are resolved on a one-electron density of states, which is dominated by the D_z states in intrinsic material. This situation is interesting, because it shows that for these parameters we essentially obtain the old picture of the density of states in intrinsic $a\text{-Si:H}$, namely a density of states dominated by a band of neutral defects, with their correlated states at an energy U_{eff} higher. The ratio of the density of charged to neu-

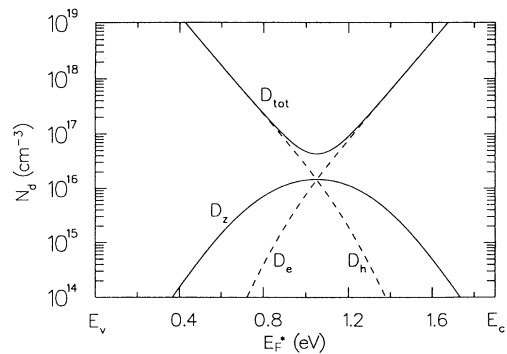


FIG. 12. The density of D_e , D_z , and D_h states as a function of Fermi level, for a narrow pool, $\sigma=0.15 \text{ eV}$.

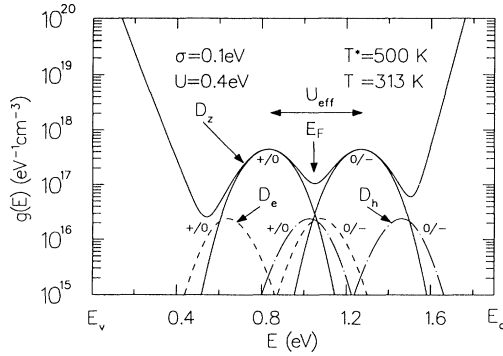


FIG. 13. One-electron density of states for a model with a very narrow pool, $\sigma=0.1$ eV, and a high correlation energy, $U=0.4$ eV.

tral defects is 0.1, so the density of D_e and D_h states is small in intrinsic material and their energy position is displaced from their position in doped material. However, a shift of the Fermi level by only 0.2 eV is required before either of the D_e or D_h states dominates (Fig. 15) and the density of states still shows the exponential increase with Fermi level, for moderate doping levels. The one-electron density of states for doped material (Fig. 14) shows resolved correlated bands of D_e states in n -type material and D_h states in p -type material. The D_e and D_h states are at different energies, but the separation is now less than the correlation energy U . The energy of the D_e^- (in n type) is 0.24 eV higher than the D_h^+ (in p type), which is clearly in contradiction to the experimental results.

COMPARISON WITH EARLIER MODELS

It is of some interest to pinpoint the exact differences between our model and those of previous work. In the original model of Bar-Yam and Joannopoulos,¹⁴ the defect formation energy for the neutral defect was an arbitrary parameter, F_0 , independent of the defect energy. The defect formation energy for charged defects was then expressed relative to that for the neutral

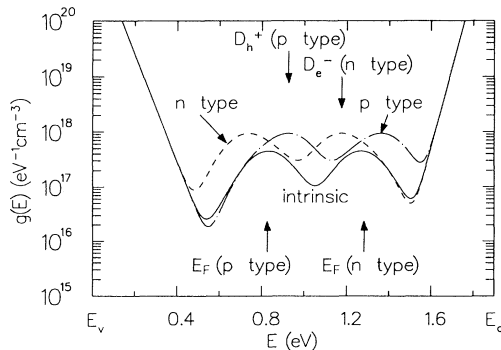


FIG. 14. One-electron density of states for lightly doped material, with a very narrow defect pool, $\sigma=0.1$ eV, and a high correlation energy, $U=0.4$ eV.

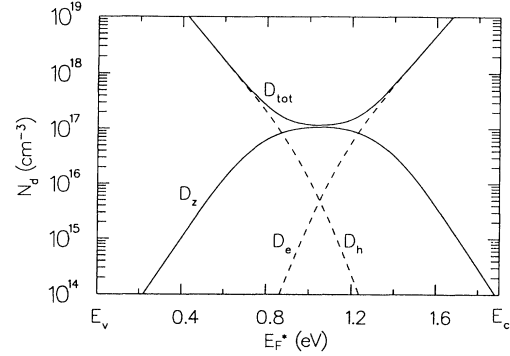


FIG. 15. The density of D_e , D_z , and D_h states as a function of Fermi level, for a very narrow pool, $\sigma=0.1$ eV, and a high correlation energy, $U=0.4$ eV.

defect. The density of formed defects was calculated from three Boltzmann expressions of the type $D(E)=N_0 \exp(-F_0/kT^*)$, where N_0 is a density of available sites, which is also a parameter. The use of this Boltzmann expression implies there is only one defect formed per chemical equilibrium reaction, though no microscopic reaction is specified. This leads to an energy separation between the D_h^+ and the D_e^- states of $2\sigma^2/kT^*-U$ and to a defect density that increases with Fermi-level shift, as $\exp(E_F/kT^*)$.

Branz and Silver²³ use the same model as Bar-Yam and Joannopoulos,¹⁴ applying it more specifically to a -Si:H. They fit the known defect densities in a -Si:H and their temperature dependence by a suitable choice of the parameters, $F_0=0.3$ eV and $N_0=10^{19}$ cm⁻³. This very low density of potential defect sites leads to severe saturation and to a resultant $D(E)$ where the peak positions of the D_h^+ states and the D_e^- states are determined by defect saturation. For the parameters given by Branz and Silver²³ ($\sigma=0.15$ eV, $kT^*=42$ meV, and $U=0.2$ eV), we calculate $2\sigma^2/kT^*-U=0.87$ eV, which would be the $D_h^+-D_e^-$ energy separation without defect saturation. With defect saturation, Branz and Silver find the energy separation to be about 0.5 eV.²³ In our model, defect saturation will only occur for the lowest energy D_e states and is masked by the valence-band-tail states. We therefore have neglected defect saturation in going from Eq. (14) to (15), in the present calculations.

In the models of Bar-Yam and Joannopoulos¹³ and Branz and Silver,²³ there is no weak-bond dangling-bond conversion, no microscopic mechanism for the defect formation process, and no specific hydrogen entropy contribution to the defect chemical potential. If hydrogen were involved, then it would be implicitly included in the F_0 term.

Winer²⁰ was the first to incorporate weak-bond dangling-bond conversion and to explicitly include hydrogen entropy in the microscopic defect formation chemical reaction. Winer²⁰ calculated the defect density assuming only one type of defect to be important for each type of material, D^0 in intrinsic, D^- in n type, and D^+ in p type. The defect chemical potential contained only one energy term in each case and no electron entropy. Hy-

drogen entropy was included, but it was calculated incorrectly, assuming each defect gained entropy from *all* Si-H sites, rather than those only at the same energy. There was also an error in the calculation of the density of D^- states in *n*-type material, because the energy scale was changed to reflect the $0/-$ transition energy, without also changing the energy scale of the defect chemical potential in a consistent way [see Ref. 20, Eq. (19), and the following sentence]. The density of D_e states was therefore underestimated. In the Winer model,²⁰ $i=1$, and the increase of the density of defects with Fermi level goes as $\exp(E_F/[E_{v0}+kT^*/2])$.

Schumm and Bauer²¹ extended the Winer model, by introducing the simultaneous formation of D_e , D_z , and D_h states. The simplest extension is to consider three *independent* chemical reactions, for the formation of dangling bonds in each charge state, from the same weak-bond states. The main error in this approach is that depletion of the weak-bond states by dangling bonds in the *other* charged states was ignored. We call this model the EW model (extended Winer). It is the model we used in our earlier work⁴¹ and is essentially the same as the "approach-I" of Schumm and Bauer.²¹ One consequence of this model is that the energy position of each of the D_e , D_z , and D_h states is fixed and the absolute density of D_z states is independent of the Fermi level. The problem with this model is that there is an inconsistency between the charge state and the occupancy of the state, which have to be treated separately.²¹

In a later paper, Schumm and Bauer²² corrected for the depletion of weak bonds by defects in all three charge states. However, they considered that the two dangling bonds should have statistically independent energies, which leads to only half the energy shift of the $+/0$ transitions of the D_e and D_z states. As previously discussed, we believe this is only correct if the defects are intimately paired. Schumm and Bauer included hydrogen entropy, but concluded that the energy spectrum of the density of

states did not change, thus the hydrogen entropy was included within a numerical scaling constant.²² We call this model the SB model (Schumm and Bauer).

Figure 16 shows the calculated ratio of charged to neutral defects that would be calculated according to the procedures of the EW and SB models. Using the same parameters as proposed by Winer,²⁰ we calculate an energy separation $D_h^+ - D_e^- = 2\sigma^2/E_{v0} - U = 0.5$ eV and a charged to neutral defect ratio of 5.7. The discrepancy with Winer's own conclusion²⁰ is due to the error in the calculation of the D_e states. This model actually predicts more charged defects than our model. The curve for the SB model is actually quite close to our model, but this is due to the approximate cancellation of two differences. The energy separation between $D_h^+ - D_e^-$ according to the SB model is $\sigma^2/E_{v0} - U$, compared to $2\rho\sigma^2/E_{v0} - U_{\text{eff}}$, in our model. For Schumm and Bauer's choice of parameters,²¹ with $i=2$, $E_{v0}=0.045$ eV, and $T^*=500$ K ($kT=0.043$ eV), then $2\rho \approx 1$, and so the shift is similar. With $\sigma=0.165$ eV,²² the SB model gives $D_h^+ - D_e^- = 0.4$ eV and a ratio of charged to neutral defects of 3.4.

DISCUSSION

In this section we compare the results of our model with other experimental results and show that the density of states we present is consistent with a wide range of experiments. An excellent discussion of the experimental evidence for charged defects has been given by Branz and Silver.²³ Here we repeat some of these arguments and present some new ones.

Figure 17 shows the calculated temperature dependence of the spin density. Above the equilibration temperature this is given by D^0 in a strongly temperature-dependent $D(E)$, but below the equilibration temperature the density of spins is only a weak function of temperature given by the temperature dependence of D^0 , within a fixed $D(E)$, as shown in Fig. 2. Above the equilibration temperature, we find that D^0 has an activation energy of 0.39 eV, which is in good agreement with 0.35 eV, found by McMahon.⁴⁷ Earlier measurements of the spin densi-

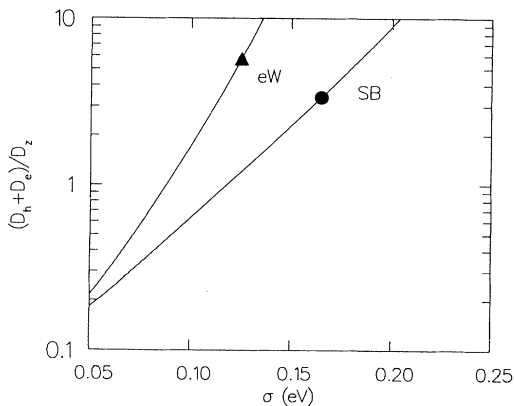


FIG. 16. Calculated charged to neutral defect ratio, at the equilibration temperature, as a function of the width of the defect pool, according to the earlier work of Refs. 20 and 22. The solid triangle indicates the position of chosen parameters in Ref. 20 and the solid circle indicates the chosen parameters in Ref. 22.

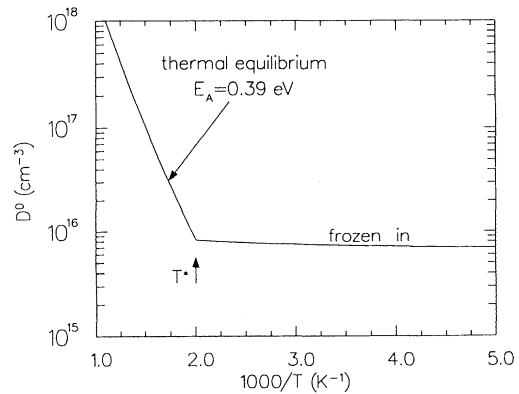


FIG. 17. Calculated temperature dependence of the spin density, D^0 , in undoped α -Si:H, above and below the freeze-in temperature, T^* .

ty above the equilibration temperature, which find a lower activation energy,³ are probably subject to systematic errors, due to the method of rapid quenching.

The weak temperature dependence of the frozen-in spin density has been analyzed recently and interpreted to give the correlation energy U .³⁶ We define the thermal modulation of the spin density as $TM = (D_{(T=300)}^0 - D_{(T=100)}^0) / 200D_{(T=100)}^0$, for comparison with experimental results.³⁶ Figure 18 shows our calculated TM plotted against σ , for different values of the correlation energy U . We note that TM is *negative* for small σ , but becomes *positive* and increases in value, as σ increases. TM is a function of U , but it also depends on σ . For the density of states in Fig. 13, TM is negative. For our parameters, we predict a positive TM of $5.8 \times 10^{-4} \text{ K}^{-1}$, compared to measured positive values in the range $(1-3) \times 10^{-4} \text{ K}^{-1}$.³⁶

The temperature dependence of the spin density comes from the positive temperature dependence of U_{eff} together with any effect of a changed occupancy in a nonconstant $D(E)$. However, this analysis makes the important assumption that U itself is not temperature dependent, which is open to question. Given that U comes from electron-electron Coulomb repulsion less any lattice relaxation energy, then we might expect the lattice relaxation energy to contribute a negative temperature dependence to TM. Since TM is very small, only a very small effect would make a significant contribution and so reduce the calculated TM.

Figure 19 represents the calculated spin density (D^0 at 313 K) as a function of the total defect density (D_{tot} frozen-in at 500 K), as we alter the material quality. We know that the density of defects increases, primarily as a result of an increase in the disorder, which leads to an increase in E_{v0} . The problem is that we do not know exactly how σ varies. In Fig. 19, we plot two extreme cases: in one case σ is constant, in the other case σ increases to keep Δ constant. In the latter case, the energy spectrum of $D(E)$ remains the same and the ratio of charged to neutral defects remains constant. However, even with

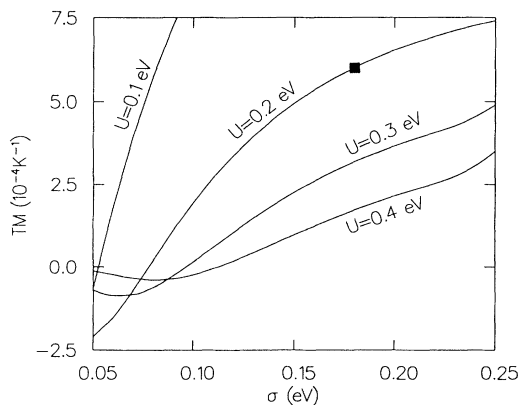


FIG. 18. The calculated thermal modulation electron-spin density, defined by $TM = (D_{(T=300)}^0 - D_{(T=100)}^0) / 200D_{(T=100)}^0$, as a function of the width of the defect pool, for different values of the correlation energy, U . The solid square indicates the result for the choice of parameters in Figs. 2-6.

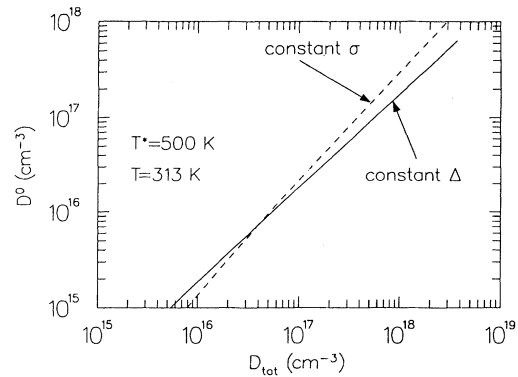


FIG. 19. The calculated spin density, D^0 at 313 K, as a function of the total density of frozen-in defects, D_{tot} , representative of different quality intrinsic a -Si:H. For both curves, E_F , U , and i are constant, while E_{v0} is varied, either with constant Δ (solid line) or constant σ (dashed line).

the most extreme assumption that σ is constant, the departure from proportionality is small. The proportionality of such a plot has been used to support the argument that the spin density measures all the defects in a -Si:H, but the experimental data from photothermal deflection spectroscopy,⁴⁸ for example, are perfectly compatible with either plot in Fig. 19.

However, the fact that *light-induced* changes in the total defect density produce a disproportionality in the spin versus total defect density is good evidence for the existence of charged defects in the annealed state.⁴⁹ It is now well established that prolonged illumination creates mainly D^0 states and therefore produces a *nonequilibrium* density-of-states distribution. Remember that all results discussed in this paper refer to an equilibrium density of states. The results of Schumm, Lotter, and Bauer⁴⁹ can be interpreted within a defect-pool model as showing a charged to neutral defect ratio of 4,⁴⁹ in excellent agreement with our results.

Cohen and co-workers have investigated the density of states in a -Si:H using depletion-width modulated electron-spin resonance (DM).^{50,51} In n -type material, the DM signal showed spin creation consistent with $D^- \rightarrow D^0$ transitions, with a positive correlation energy $> 0.2 \text{ eV}$.⁵⁰ However, in undoped a -Si:H they found a negligible DM signal, which they interpreted as showing zero correlation energy.⁵¹ Branz and Silver²³ and Lee and Schiff³⁶ pointed out that a zero DM signal is to be expected in true intrinsic material, but this is only true for small displacements of the Fermi level. Our density of states predicts that the DM signal will be negligible for relatively large displacements of the Fermi level through the frozen-in density of states for intrinsic material. This is because the total $g(E)$ is relatively flat and there will be an equal number of $D^0 \leftrightarrow D^-$ and $D^+ \leftrightarrow D^0$ transitions. The defect-pool model, with charged defects, is therefore consistent with these observations.

Chen and co-workers have investigated the density of states in a -Si:H, using photomodulation spectroscopy.³⁹ Their fitting of the photomodulation spectrum (PM) leads

to assignments of the energy positions of the defect states. For n -type a -Si:H, they detect (in our notation) $D_e^{0/-}$ and $D_e^{+/0}$, separated by 0.25 eV, which is therefore the correlation energy U . Note that the optical transition energies, not the thermal transition energies, will be observed in this technique. In p -type material, they detect $D_h^{+/0}$, which is found 0.4 eV higher than the $D_e^{0/-}$ level in n -type material. This compares well with the $\Delta=0.44$ eV energy separation, in our model. In intrinsic material, Chen and co-workers observe two transitions, which they assign to D_z levels (assuming these to be dominant as in a conventional model of a -Si:H, like Fig. 13) and conclude that the correlation energy in intrinsic material is 0.6 eV. However, in our model, with dominant charged defects, we would expect to see the same transition energies as either the n - or p -type material. This is exactly what is observed with the PM spectra picking out the same features as observed in p -type material, apart from the impurity band transitions. The interpretation of the energy separation of these transition energies in our model is $\Delta+0.2$ eV=0.64 eV, which agrees well with the observations. The PM results therefore support our model with a dominance of charged defects in intrinsic material.

Further evidence for the presence of charged defects in intrinsic a -Si:H is contained in some LESR (Ref. 52) and infrared LESR (Ref. 53) measurements. However, there are contradictory reports on the lack of any defect ($g=2.0055$) LESR (Ref. 54) and even of LESR quench-

ing.^{54,55} The fact that LESR quenching can ever be observed means that not *all* defects are converted to D^0 states on illumination and so there is the possibility that some charged defects may not be detected or may be masked by the band-tail signals.

CONCLUSIONS

The essential thesis of this paper is that the density of dangling-bond states in amorphous silicon is determined by a chemical equilibrium process and on this basis it is possible to calculate, analytically, the density-of-states distribution. The result depends on several parameters, which can be found from experimental results. Better precision is needed in a number of these parameters, but using the best available data from a wide range of experiments, we calculate a density of states for intrinsic a -Si:H with approximately four times as many charged defects as neutral defects.

ACKNOWLEDGMENTS

The authors thank C. van Berkel for many early discussions of the defect-pool model and several important contributions to this work. We have benefited from stimulating discussions on the evidence for and against charged defects with R. A. Street, M. Stutzmann, and J. Robertson. We also thank J. Robertson for a critical reading of the manuscript.

-
- ¹R. A. Street, J. Kakalios, C. C. Tsai, and T. M. Hayes, *Phys. Rev. B* **35**, 1316 (1987).
²R. A. Street, M. Hack, and W. B. Jackson, *Phys. Rev. B* **37**, 4209 (1988).
³R. A. Street and K. Winer, *Phys. Rev. B* **40**, 6236 (1989).
⁴M. Stutzmann, *Philos. Mag.* **B 56**, 63 (1987).
⁵G. Muller, *Appl. Phys. A* **45**, 41 (1988).
⁶R. S. Crandall, *Phys. Rev. B* **43**, 4057 (1991).
⁷G. Muller, S. Kalbitzer, and H. Mannsperger, *Appl. Phys. A* **39**, 250 (1986).
⁸L. Ley and K. Winer, *Proceedings of the International Conference on the Physics of Semiconductors* (Polish Institute of Physics, Warsaw, 1989), p. 1633.
⁹K. Winer, *Phys. Rev. Lett.* **63**, 1487 (1989).
¹⁰Z. E. Smith and S. Wagner, in *Amorphous Silicon and Related Materials*, edited by H. Fritzsche (World Scientific, Singapore, 1989), p. 409.
¹¹J. Kocka, M. Vanacek, and F. Schauer, *J. Non-Cryst. Solids* **97&98**, 715 (1987).
¹²K. Winer, I. Hirabayashi, and L. Ley, *Phys. Rev. B* **38**, 7680 (1988).
¹³K. Pierz, W. Fuhs, and H. Mell, *Philos. Mag.* **B 63**, 123 (1991).
¹⁴Y. Bar-Yam and J. D. Joannopoulos, *J. Non-Cryst. Solids* **97&98**, 467 (1987).
¹⁵Z. E. Smith and S. Wagner, *Phys. Rev. Lett.* **59**, 688 (1987).
¹⁶J. Kakalios, R. A. Street, and W. B. Jackson, *Phys. Rev. Lett.* **59**, 1037 (1987).
¹⁷W. B. Jackson, *Phys. Rev. B* **41**, 10257 (1990).
¹⁸R. A. Street, *Phys. Rev. B* **43**, 2454 (1991).
¹⁹W. B. Jackson and C. C. Tsai, *Phys. Rev. B* **45**, 6564 (1992).
²⁰K. Winer, *Phys. Rev. B* **41**, 12150 (1990).
²¹G. Schumm and G. H. Bauer, *Philos. Mag.* **B 64**, 515 (1991).
²²G. Schumm and G. H. Bauer, *J. Non-Cryst. Solids* **137&138**, 315 (1991).
²³H. M. Branz and M. Silver, *Phys. Rev. B* **42**, 7420 (1990); in *Amorphous Silicon Technology—1990*, edited by P. C. Taylor, M. J. Thompson, P. G. LeComber, Y. Hamakawa, and A. Madan, MRS Symposia Proceedings No. 192 (Materials Research Society, Pittsburgh, 1990), p. 261.
²⁴S. C. Deane and M. J. Powell, *Phys. Rev. Lett.* **70**, 1654 (1993).
²⁵See, for example, C. Kittel, *Thermal Physics* (Wiley, New York, 1969), p. 143.
²⁶H. Okamoto and Y. Hamakawa, *Solid State Commun.* **24**, 23 (1977).
²⁷*Thermal Physics* (Ref. 25), p. 118.
²⁸The integral in Eq. (14) can be solved exactly, with the result that the factor $2E_{v0}^2/[2E_{v0}-kT]$ in Eqs. (15) and (18) is replaced by $\pi kT/\{2\sin(\pi kT/[2E_{v0}])\}$. This leads to a correction in the total density of states of about 12%, which is less than the experimental uncertainty in input parameters, e.g., N_{v0} and H , which have the same effect.
²⁹I. Hirabayashi, K. Winer, and L. Ley, *J. Non-Cryst. Solids* **97-98**, 87 (1987).
³⁰C. R. Wronski, S. Lee, M. Hicks, and Satyendra Kumar, *Phys. Rev. Lett.* **63**, 1420 (1989).
³¹M. Stutzmann, *Philos. Mag. Lett.* **66**, 147 (1992).
³²M. Vanacek, B. P. Nelson, A. H. Mahan, and R. S. Crandall,

- J. Non-Cryst. Solids **137-138**, 191 (1991).
- ³³H. Dersch, J. Stuke, and J. Beichler, *Phys. Status Solidi B* **105**, 265 (1981).
- ³⁴W. B. Jackson, *Solid State Commun.* **44**, 477 (1982).
- ³⁵M. Stutzmann and W. B. Jackson, *Solid State Commun.* **62**, 153 (1987).
- ³⁶J.-K. Lee and E. A. Schiff, *Phys. Rev. Lett.* **68**, 2972 (1992).
- ³⁷S. C. Deane and M. J. Powell (unpublished).
- ³⁸R. A. Street and D. K. Biegelsen, *Solid State Commun.* **33**, 1159 (1980).
- ³⁹L. Chen, J. Tauc, J. Kocka, and J. Stuchlik, *Phys. Rev. B* **46**, 2050 (1992).
- ⁴⁰K. Winer, I. Hirabayashi, and L. Ley, *Phys. Rev. B* **38**, 7680 (1988).
- ⁴¹M. J. Powell, C. van Berkel, A. R. Franklin, S. C. Deane, and W. I. Milne, *Phys. Rev. B* **45**, 4160 (1992).
- ⁴²R. L. Weisfield, *J. Appl. Phys.* **54**, 6401 (1983).
- ⁴³D. V. Lang, J. D. Cohen, and J. P. Harbison, *Phys. Rev. B* **25**, 5285 (1982).
- ⁴⁴J. D. Cohen, *J. Non-Cryst. Solids* **114**, 381 (1989).
- ⁴⁵M. J. Powell and J. Pritchard, *J. Appl. Phys.* **54**, 3244 (1983).
- ⁴⁶M. Stutzmann, D. K. Biegelsen, and R. A. Street, *Phys. Rev. B* **35**, 5666 (1987).
- ⁴⁷T. J. McMahon, in *Amorphous Silicon Materials and Solar Cells*, edited by B. L. Stafford, AIP Conf. Proc. No. 234 (AIP, New York, 1991), p. 83.
- ⁴⁸W. B. Jackson and N. M. Amer, *Phys. Rev. B* **25**, 5559 (1982).
- ⁴⁹G. Schumm, E. Lotter, and G. H. Bauer, *Appl. Phys. Lett.* **60**, 3262 (1992).
- ⁵⁰J. D. Cohen, J. P. Harbison, and K. W. Wecht, *Phys. Rev. Lett.* **48**, 109 (1982).
- ⁵¹J. M. Essick and J. D. Cohen, *Phys. Rev. Lett.* **64**, 3062 (1990).
- ⁵²T. Shimizu, H. Kidoh, A. Morimoto, and M. Kumeda, *Jpn. J. Appl. Phys.* **28**, 586 (1989).
- ⁵³H. M. Branz, *Phys. Rev. B* **41**, 7887 (1990).
- ⁵⁴M. Stutzmann (private communication); see also M. Brandt, A. Asano, and M. Stutzmann in *Amorphous Silicon Technology-1993*, MRS Symposia Proceedings No. 297 (Materials Research Society, Pittsburgh, in press).
- ⁵⁵A. Friedrich and D. Kaplan, *J. Non-Cryst. Solids* **35-36**, 657 (1980).